Article

Research on a Comprehensive Evaluation Method of Train Anti-Slip System Performance

Gaowei Zhou [1,2], Hongfeng Qi [2], Hao Yu [3], Jiajun Zhou [3,*] and Fei Gao [1]

[1] Engineering Research Center of Continuous Extrusion, Ministry of Education, Dalian Jiaotong University, Dalian 116028, China; zhougaowei@crrcgc.cc (G.Z.)

[2] CRRC Industrial Academy Corporation Limited, Beijing 100070, China

[3] Institue of Rail Transit, Tongji University, Shanghai 201804, China; 2131399@tongji.edu.cn

* Correspondence: 892149508@tongji.edu.cn; Tel.: +86-15317915220

Abstract: The quality of a train's braking anti-slip control system has a significant impact on train safety and braking performance. Currently, there is no established standard evaluation method for anti-slip control systems, making it an important area of research in the academic community. This article comprehensively considers four key indexes: adhesive coefficient utilization rate, air consumption increase ratio, wheel slip work, and anti-slip valve action frequency. The evaluation system takes into account the influence of load layer and braking level, and proposes a comprehensive evaluation method for train anti-slip control based on multi-factor hierarchical analysis. A series of experiments were conducted using a semi-physical simulation test bench for anti-slip evaluation, aimed at comprehensively evaluating two different anti-slip control strategies. By applying the method proposed in this article, the above four indexes and their corresponding weights of two anti-slip control strategies under different conditions were calculated. Finally, the comprehensive evaluation result R1 of anti-slip control strategy 1 was calculated as 0.8389, while the comprehensive evaluation result R2 of anti-slip control strategy 2 was calculated as 0.7912. Based on the comprehensive evaluation results, it is evident that the anti-slip comprehensive evaluation method established in this article is comprehensive and scientific, with concise and clear evaluation results. This method carries certain reference significance for the design of future anti-slip evaluation methods.

Keywords: train braking; semi-physical simulation; anti-slip evaluation

1. Introduction

The train braking system is an integral component of the railway vehicle system, and the anti-slip system, as one of its key subsystems, plays a vital role in ensuring braking performance under low adhesion conditions. Therefore, it is an ongoing challenge to effectively evaluate the performance of anti-slip systems.

Currently, the performance evaluation of train anti-slip devices is primarily based on national regulations in practical applications. The relevant railway standards in Europe and China have put forward clear requirements for the performance and function of train devices [1–3]. For example, most European countries adopt the EN15595 standard [1] and UIC CODE 541-05 [2] standard, which mainly focus on the evaluation methods and standards for the performance and safety of train anti-slip devices, while China mainly adopts the TB/T 3009 standard [3]. However, the various indexes required to test the performance of anti-slip devices are all single qualification requirements, with a focus on evaluating the braking distance indexes during operation of the anti-slip devices. The concept of anti-slip efficiency is proposed in the technical specifications for Shanghai Metro Line 1, referring to the ratio of the ideal shortest stopping distance of the anti-slip system to the actual running stopping distance under given working conditions (adhesion coefficient of 0.05–0.08, speed above 8 km/h) [4]. The higher the anti-slip efficiency, the better the

performance of the anti-slip system. Regarding the practical application of the concept of anti-slip efficiency, Wu Zhiwei and Hu Yongsheng et al. proposed several different calculation methods for anti-slip efficiency in their article [4]. Chen Wei et al. applied the deceleration linear assumption calculation method to analyze and process test data from actual anti-slip tests on CRH3 multiple units and found that the anti-slip efficiency during pure air emergency braking was about 105%, with an efficiency value greater than 100%. This indicates that there are still many difficulties in calculating anti-slip efficiency in actual vehicle slipping tests [5,6]. At present, it is difficult to accurately evaluate the train anti-slip system using a single index. Therefore, some scholars have proposed a more comprehensive and scientific evaluation method for train anti-slip performance. The authors of [7] propose a statistical evaluation method for train anti-slip performance based on braking distance and randomly changed the amplitude and frequency of the adhesive coefficient curve within a certain range to conduct statistical evaluation of anti-slip control algorithms under different adhesive conditions. The method has a certain innovation, but it is simplistic to evaluate train anti-slip performance through braking distance only, making it difficult to comprehensively consider train anti-slip performance. The authors of [8] used dispersion standardization to normalize and standardize various indexes, and obtained a set of performance evaluation methods for train anti-slip systems based on the analytic hierarchy process. However, the influence of brake level and train load changes on anti-slip performance was ignored in the text, which also made it difficult to accurately reflect the performance of train anti-slip systems in the evaluation results.

In summary, many scholars have conducted research on the performance evaluation methods of train anti-slip systems. Some only consider anti-slip efficiency or braking distance, while others establish anti-slip evaluation systems through comprehensive evaluation methods, but ignore the influence of load and braking level. Therefore, this article comprehensively considers the adhesive coefficient utilization index, air consumption increase ratio index, wheelset slipping energy index, and anti-slip valve action frequency index. The analytic hierarchy process was used to establish a comprehensive performance evaluation system for the anti-slip system, and the train load layer and brake level layer were added. Based on the semi-physical simulation platform of anti-slip control which was verified by EN15595 [1], performance testing of the anti-slip control strategy was carried out. Based on the optimized anti-slip system performance evaluation method, experimental data were calculated and processed to obtain comprehensive performance evaluation results, thereby verifying the application effect of the evaluation method on the semi-physical simulation platform.

2. Anti-Slip Performance Evaluation Indexes

The performance evaluation system developed in this article for train anti-slip systems includes four indices: an adhesive coefficient utilization index, an air consumption increase ratio index, a wheelset slip energy index, and an anti-slip valve action frequency index, as depicted in Figure 1. The adhesive coefficient utilization index directly reflects the utilization of wheel–rail adhesive by the train anti-slip controller, which directly impacts train braking distance, average deceleration, and the like. The air consumption of the brake cylinder indicates the load size of the braking system on the air source during the braking process. To eliminate differences in air consumption resulting from the inherent characteristics of the system, this article assesses the increased ratio of air consumption under different wheel–rail adhesive levels relative to dry rail braking air consumption. The lower the increase in the ratio of air consumption under the same adhesive level, the higher the economic efficiency. The wheelset slip energy index is obtained from the formula for wheel–rail wear power established by the speed difference and adhesion of the wheelset. A lower value indicates a smaller degree of wheel–rail wear during the slip control process, and a lower probability of wheel scuffing, abnormal vehicle vibration, and serpentine motion. Finally, the anti-slip valve action frequency index directly affects the service life of the anti-slip valve.
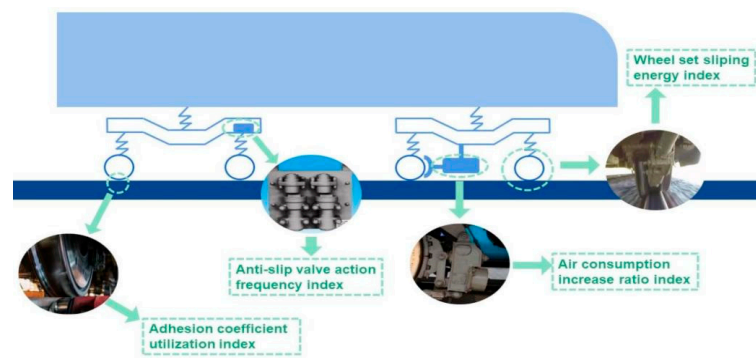
Figure 1. Evaluation indexes of anti-slip performance.

2.1. Adhesion Coefficient Utilization Index

The actual adhesive coefficient refers to the adhesive coefficient value actually utilized during the train braking process. In practical train testing, both the maximum adhesive coefficient available and the actual adhesive coefficient cannot be directly measured, and can only be estimated through instantaneous train deceleration or other parameters, making it difficult to obtain an accurate value. However, in the semi-physical simulation platform test, the adhesive coefficient is usually simulated by a numerical simulation model. Therefore, the wheel–rail adhesive coefficient during the entire train braking and anti-skid process and the actual adhesive coefficient can be easily obtained, making it possible to accurately calculate the adhesive coefficient utilization under anti-slip control.

Assuming that the anti-slip system can always maximize the utilization of adhesion during the braking process—that is, the adhesive coefficient is always the maximum—from this, the theoretical shortest braking distance is calculated, and the actual braking distance is obtained through testing. Therefore, the adhesive coefficient utilization during the entire braking process of the train is as follows:

$$\eta = \frac{s_{\min}}{s_{\text{real}}} \times 100\% \tag{1}$$

Due to the different dimensions and magnitudes of different evaluation indexes, it is necessary to normalize them so that the index results are in the same order of magnitude for comprehensive evaluation in conjunction with the analytic hierarchy process. Here, the deviation standardization method is used to map the index results to 0–1. The calculation method for standardization of dispersion is as follows:

$$x^* = \frac{x - x_{\min}}{x_{\max} - x_{\min}}, x^* = 1 - \frac{x - x_{\min}}{x_{\max} - x_{\min}} \tag{2}$$

Formula (2) represents two forms of deviation standardization, both of which are used in this article. x^* represents the standardized deviation index, $x_{\max}$ represents the maximum value of the index, $x_{\min}$ represents the minimum value of the index, and x represents the calculated value of the index.

For the adhesion coefficient utilization index throughout the braking process, take the minimum value $\eta_{\min} = 0$ to represent the wireless extension of braking distance. The maximum value $\eta_{\max} = 100\%$ indicates that the anti-slip system can fully utilize the adhesion coefficient and has the shortest braking distance. The normalized index is as follows:

$$x_1 = \frac{\eta - 0}{100\% - 0} \tag{3}$$

2.2. Air Consumption Increase Ratio Index

Due to differences in brake cylinder size, pipe diameter, pipeline length, target brake cylinder pressure, etc., in different braking systems, in order to eliminate the impact of different air consumption caused by the inherent characteristics of the system itself, the air consumption increase ratio relative to the dry rail working condition is used as the calculation index. The air consumption under dry rail conditions is V_{dry} and the air consumption under slipping conditions is V_{slip}; therefore, the calculation formula for the air consumption increase ratio k is as follows:

$$k = \frac{V_{slip}}{V_{dry}} \tag{4}$$

For the air consumption increase ratio index, take the minimum value $k_{min} = 1$, indicating that the air consumption under anti-slip control has not increased compared to when the dry rail is not slipping. The maximum value $k_{max} = V_{cr}$. The value of V_{cr} refers to the requirements of Annex B of EN15595 for the air consumption limit of anti-slip device simulation platform testing at different initial braking speeds [1]. The standard only describes the allowable maximum relative air consumption for braking initial speeds below 160 km/h. In order to meet the performance testing and evaluation requirements of the anti-slip system at higher speeds, this article expands the relationship between the air consumption increase ratio and the braking initial speed based on the original provisions in the standard. As shown in Table 1 below, the normalized index x_2 is as follows:

$$x_2 = 1 - \frac{k - 1}{V_{cr} - 1} \tag{5}$$

Table 1. Limit value of air consumption increase ratio under different initial braking speeds.

Initial Braking Speed V_0 (km/h)	V_{cr}
40	15
80	20
120	25
⋮	⋮
350	55

2.3. Wheelset Slipping Energy Index

The slip energy of the wheelset is mainly generated by the speed difference between the wheels and rails. The slip energy value affects the degree of wear on the wheel tread and track surface, and excessive wear can cause wheel–rail scratches. Define the wear power P as [9]:

$$P = \mu \times T \times \Delta v \tag{6}$$

where μ is the actual utilized adhesion coefficient, T is the positive pressure between the wheel and rail (unit: N), and Δv is the speed difference between the wheel and rail (unit: m/s). Therefore, the wheelset slip energy W (unit: J) is as follows [9]:

$$W = \int \mu \times T \times \Delta v dt \tag{7}$$

Starting from the start of the pressure maintaining valve in the anti-slip valve and ending with the stop of the pressure maintaining valve as a slipping control cycle, during which the train is in a slipping control state, the wheelset slipping energy during each slipping cycle W_i is calculated, and the average value of the wheelset slipping energy for a single axle during the entire braking anti-slip process W_{avg} is calculated. Then, the average

value of the wheelset slipping energy is taken as the index of the wheelset slipping energy for all axles.

$$W_{avg} = \frac{\sum_1^n W_i}{n} (i = 1, 2, 3, \ldots n), n \text{ is the number of single axis slipping cycles} \quad (8)$$

$$W = \frac{\sum_1^m W_{mavg}}{m}, m \text{ is the number of slipping axles} \quad (9)$$

For the wheelset slipping energy index, the minimum value is taken as $w_{min} = 0$. At this time, the train wheelset is in a pure rolling state, and there is no speed difference or wear between the wheels and rails. The maximum value is taken as $w_{max} = 26,000$ J. This value is taken from the requirement in EN15595 that the wheelset slipping energy during a single slipping cycle should not exceed 26 kJ [1]. The normalized index x_3 is as follows:

$$x_3 = 1 - \frac{w - 0}{26,000 - 0} \quad (10)$$

2.4. Anti-Slip Valve Action Frequency Index

Due to the stage charging and discharging strategy, the number of actions of the exhaust valve must not be less than the number of actions of the pressure maintaining valve, and even when the adhesion conditions are severe, there will be 3–5 exhausts within a slipping cycle, making the former action times much greater than the latter. Therefore, the exhaust valve can better reflect the usage frequency of the anti-slip valve by the anti-slip system, so this index only needs to count the number of actions of the exhaust valve. Record the driving signal of the solenoid valve from low to high and then to low (0-1-0) as one action, and count r_i, which is the number of actions of the exhaust valves on each axle during the entire braking process under slipping conditions, and calculate the average value h_{avg} as anti-slip valve action frequency index.

$$h_{avg} = \frac{\sum_1^m r_i}{m} (i = 1, 2, 3 \ldots, m), m \text{ is the number of slipping axles} \quad (11)$$

For the anti-slip valve action frequency index, take the minimum as $h_{min} = 0$ and the maximum as h_{max} (refer to simulation tests and actual vehicle test data for the anti-slip valve action, which is related to the initial braking speed, and h_{max} shown in Table 2); then, the normalized index x_4 is as follows:

$$x_4 = 1 - \frac{h_{avg} - 0}{C - 0} \quad (12)$$

Table 2. Values under different initial braking speeds.

Initial Braking Speed V_0 (km/h)	h_{max}
120	300
150	400
200	500
250	600
350	800

3. Optimization of Train Anti-Slip Evaluation Method

Factors such as train load and braking level have a certain impact on the anti-slip performance of trains, but they have not been fully considered in the current evaluation methods of train anti-slip system performance. Therefore, this article establishes an optimized hierarchical structure model of the anti-slip performance evaluation system for this purpose. The first layer is the anti-slip performance, which is the target layer, the second layer is for train load, the third layer is for braking level, the fourth layer is for

adhesion conditions, and the fifth layer is for anti-slip performance indexes, all of which are criterion layers.

3.1. Hierarchy of Anti-Slip Evaluation System

The analytic hierarchy process (AHP) refers to the systematic method of decomposing a complex multi-objective decision-making problem into multiple objectives or criteria as a system, and then decomposing them into multiple levels of multiple indicators (or criteria, constraints). By using qualitative indicator fuzzy quantification methods, the hierarchical single ranking (weight) and total ranking are calculated, which serve as the objective (multiple indicators) and multi-scheme optimization decision-making system. This article required the use of four anti-slip performance indexes to evaluate the performance of train anti-slip devices. The analytic hierarchy process (AHP) has advantages for such multi-objective decision-making problems. The evaluation system established using AHP can effectively integrate various indexes, making it an excellent method for the problem studied in this article.

According to the usage method and requirements of the analytic hierarchy process, it is necessary to compare the importance of each layer element in pairs, establish a judgment matrix, and quantitatively obtain the weight proportion of each layer element. The judgment matrix was constructed using the 1–9 scale method shown in Table 3 [10].

Table 3. Judgment matrix scale and its meaning.

Scale	Meaning
1	Indicates that two factors are equally important compared to each other.
3	Indicates that compared to two factors, one factor is slightly important compared to the other.
5	Indicates that compared to two factors, one factor is significantly important compared to the other.
7	Indicates that compared to two factors, one factor is strongly important compared to the other.
9	Indicates that compared to two factors, one factor is extremely important compared to the other.
2, 4, 6, 8	The median of the two adjacent judgments mentioned above.
reciprocal	Comparing factor i with j yields a judgment of b_{ij}, then comparing factor j with i yields a judgment of b_{ji}.

When selecting the scaling values of the judgment matrix elements in the analytic hierarchy process, in order to maintain the consistency of the decision-maker's judgment thinking, it is necessary to test the consistency of the judgment matrix; that is, the judgment matrix A needs to meet the following relationship:

$$a_{ij} = \frac{a_{ik}}{a_{jk}} \; ; \; i, j, k = 1, 2, 3, \ldots \ldots, n \tag{13}$$

According to matrix theory, it is determined that a matrix has a unique, non zero, and maximum eigenvalues $\lambda_{\max} = n$, and all other eigenvalues except for $\lambda_{\max}$ are 0 under the conditions of complete consistency mentioned above. Therefore, in the application of the analytic hierarchy process, the solution of the characteristic roots and eigenvectors of the judgment matrix is crucial. This article uses the square root method. The process of calculating the weights and maximum feature roots of each element using the square root method is as follows:

(1)   Calculate the product of each row of the judgment matrix, where n is the matrix order:

$$M_i = \prod_{j=1}^{n} b_{ij} \, , i = 1, 2, 3, \ldots \ldots, n \tag{14}$$

(2)   Calculate the nth root of M_i for each row:

$$\overline{w}_i = \sqrt[n]{M_i}, i = 1, 2, 3, \ldots \ldots, n \tag{15}$$

(3) Normalize vector $\left(\overline{M}_1, \overline{M}_2, \overline{M}_3...\right)^{\mathrm{T}}$, and w_i is the weight coefficient of each index:

$$w_i = \frac{\overline{w}_i}{\sum_{j=1}^{n} \overline{w}_j} \tag{16}$$

(4) The maximum eigenvalue of the judgment matrix is:

$$\lambda_{max} = \sum_{i=1}^{n} \frac{(AW)_i}{nw_i} \tag{17}$$

(5) Calculate the consistency index CI and consistency ratio CR, and verify whether the judgment matrix has satisfactory consistency. $CI = \frac{\lambda_{max} - n}{n-1}$, $CR = \frac{CI}{RI}$, RI is the average random consistency index, and its values are shown in Table 4. The condition for good consistency of the judgment matrix is $CR < 0.1$, otherwise it needs to be adjusted.

Table 4. Average random consistency index RI.

n	1	2	3	4	5	6	7	8	9	10	11	12	13
RI	0	0	0.52	0.89	1.12	1.26	1.36	1.41	1.46	1.49	1.52	1.54	1.56

3.2. Judgment Matrix at Each Level

For the train load layer, this layer contains two elements: fully loaded and unloaded. Under the same rail surface conditions, the probability of a train sliding under full load conditions and the difficulty of sliding control are higher than under no-load conditions. Therefore, the anti-slip performance test results of the former are more important than those of the latter. The judgment matrix is shown in Table 5, where A1 represents the AW3 full load condition and A2 represents the AW0 no load condition. Calculate the weight coefficients of the two elements based on this judgment matrix, and the results are A1 = 0.67, A2 = 0.33. The consistency check result CR = 0 < 0.1 meets the requirements.

Table 5. Train load layer judgment matrix.

A	A1	A2
A1	1	2
A2	0.5	1

The braking level layer contains two elements: emergency braking and maximum service braking. Emergency braking reflects the safety of the train's anti-slip braking process under emergency conditions, while maximum service braking reflects the safety of the train's anti-slip braking process under general conditions, both of which have the same importance. The judgment matrix is shown in Table 6, where B1 represents the emergency braking conditions and B2 represents the maximum service braking conditions. The weight calculation results are B1 = 0.5, B2 = 0.5. The consistency verification result = 0 < 0.1, meeting the requirements.

Table 6. Brake level layer judgment matrix.

B	B1	B2
B1	1	1
B2	1	1

The wheel–rail adhesion condition layer contains four elements, which are the maximum adhesion coefficients 0.05, 0.06, 0.07, and 0.08. Based on the comparison of the probability of encountering corresponding adhesion level working conditions during actual train operation, and referring to the probability of various weather conditions that may cause low adhesion of wheels and rails, the judgment matrix established is shown in Table 7 where C1, C2, C3, and C4 respectively represent a 0.05 maximum adhesion level, a 0.06 maximum adhesion level, a 0.07 maximum adhesion level, and a 0.08 maximum adhesion level. The weight coefficient results are C1 = 0.0809, C2 = 0.1539, C3 = 0.2880, and C4 = 0.4773. The consistency verification result = 0.0079 < 0.1, meeting the requirements.

Table 7. Adhesion condition layer judgment matrix.

C	C1	C2	C3	C4
C1	1	1/2	1/4	1/5
C2	2	1	1/2	1/3
C3	4	2	1	1/2
C4	5	3	2	1

The anti-slip performance index layer includes four elements: adhesion coefficient utilization index, air consumption increase ratio index, wheelset slipping energy index, and anti-slip valve action frequency index. The judgment matrix established from this is shown in Table 8, where D1, D2, D3, and D4 respectively represent the adhesion coefficient utilization, air consumption increase ratio, wheelset slipping energy, and the anti-slip valve action frequency. The weight coefficient results are D1 = 0.4231, D2 = 0.2272, D3 = 0.2272, D4 = 0.1225. The consistency check result CR = 0.0039 < 0.1 meets the requirements.

Table 8. Judgment matrix of anti-slip performance index layer.

D	D1	D2	D3	D4
D1	1	2	2	3
D2	1/2	1	1	2
D3	1/2	1	1	2
D4	1/3	1/2	1/2	1

*3.3. Comprehensive Evaluation Results of Anti-Slip Performance*

The above content completes the improvement and optimization of the original anti-slip system performance evaluation method. According to Figure 2, the optimized evaluation method describes the calculation process of the comprehensive evaluation method of train anti-slip system performance:

(1) Complete the required tests according to the evaluation method, including fully loaded and unloaded, emergency braking and maximum service braking, and train anti-slip system performance tests under various working conditions under different adhesion coefficient cross combinations, and obtain test data.

(2) According to the qualification requirements specified in the EN15595, the test data shall be processed and analyzed to ensure that the test results of all working conditions meet the standard requirements before proceeding to the next evaluation. Otherwise, the anti-slip system shall be deemed unqualified.

(3) Calculate the results of four performance indexes under each set of working conditions, combined with the weight coefficients of each layer of elements calculated in the previous section, and obtain the values of the upper layer of elements from bottom to top. Finally, calculate the comprehensive evaluation result R of train anti-slip performance.
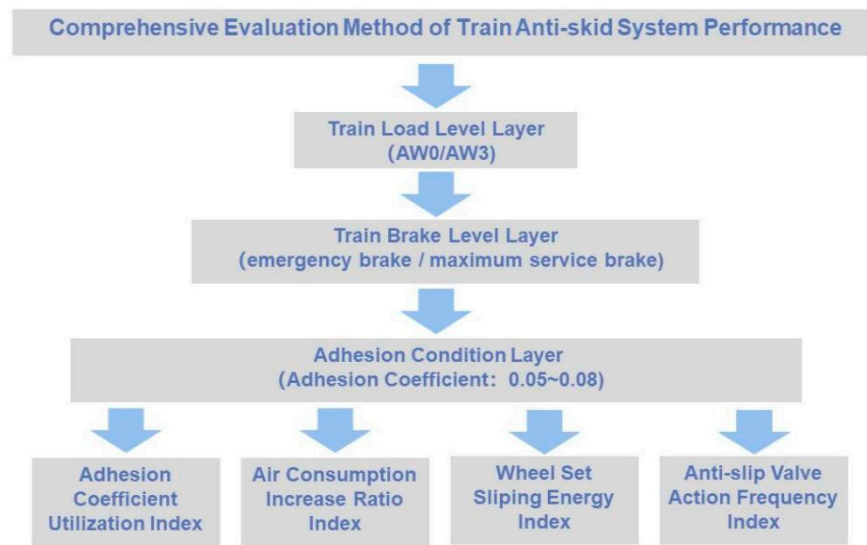
Figure 2. Comprehensive evaluation method of train anti-slip system performance.

4. Construction of a Comprehensive Test Platform for Anti-Slip Evaluation

4.1. Topology Design

According to the design requirements of the Class 2A anti-slip test platform in EN15595, the anti-slip control unit and air braking system should be hardware objects. The system should be designed based on a two-car formation of 1M1T (one motor vehicle and one trailer), and the test objects on the test platform should cover the braking system of the motor train, train frame control braking system, anti-slip control algorithm, and valve components in the air braking system. The overall plan of the comprehensive test platform for anti-slip evaluation is shown in Figure 3, and the actual platform is shown in Figure 4.
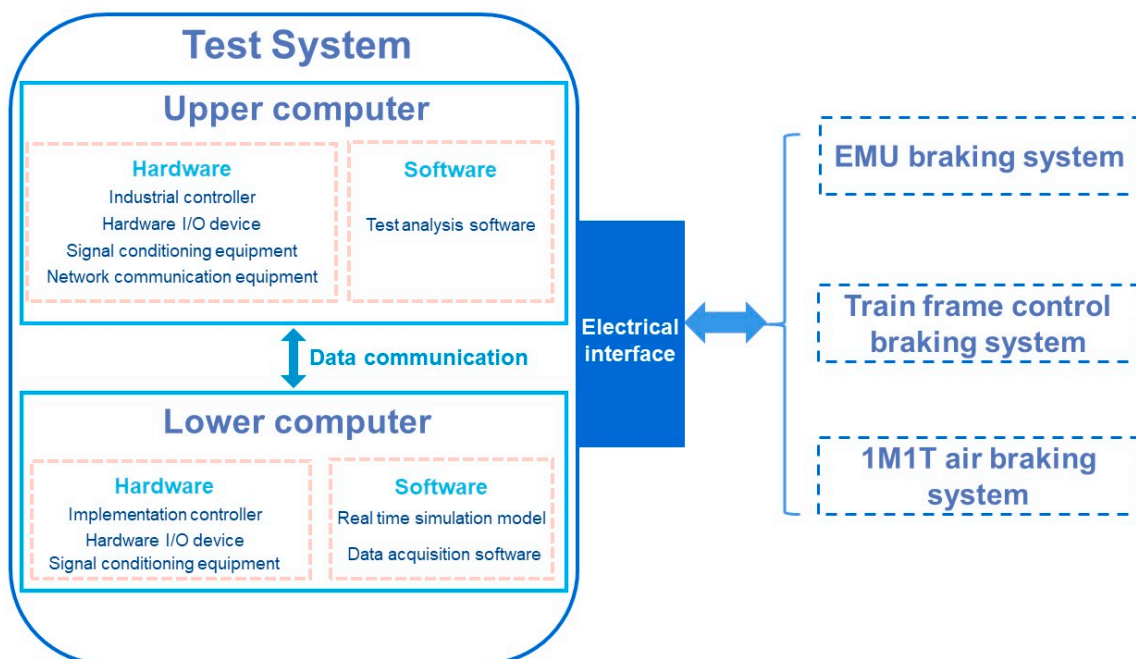
Figure 3. Overall plan.

Figure 4. The actual platform.

4.2. Hardware Design

The hardware part of the comprehensive anti-slip evaluation test platform mainly included four parts: the hardware parts of the upper and lower computers, the mechanical part, and the 1M1T air brake system. The hardware part of the upper computer consisted of an industrial control computer, data acquisition equipment, network communication equipment, etc.

The data acquisition equipment was used to generate and collect hard wire signals required for information exchange with the braking system, such as braking level signals, braking status, release status, etc. In order to cover the electrical interface signal requirements of different braking systems, a certain number of signal channels were reserved for future expansion. In addition to hard wire signals, signal transmission between the test platform and the braking system should also be possible through the MVB network. In addition, the frame controlled train also used a CAN network for communication between various EBCUs, achieving the management and distribution of braking force. The lower computer was mainly to perform simulation calculation functions, and needed high requirements for real-time accuracy of the system. Therefore, the NI PXI system was adopted for implementation.

The entire system of the comprehensive test platform for anti-slip evaluation consisted of an air source and processing device, main air cylinder, T-car plate-connected air brake control unit (PBCU), M-car plate-connected air brake control unit (PBCU), anti-slip valve, brake cylinder, and sensor, as shown in Figure 5. The PBCU was designed based on the actual vehicle system, simplifying some valve components and pipeline lengths.

In addition, due to the input signal requirements of the semi-physical simulation test platform, air pressure sensors and flow sensors were added at the corresponding nodes of the air braking system to measure key pressure signals and the air consumption during the braking anti-slip process. The arrangement nodes of the pressure sensor included the rear end of the main air cylinder, the rear end of the EP valve, the rear end of the relay valve, and the rear end of the anti-slip valve; the flow sensor was arranged between the main air cylinder and the PBCU of each vehicle.

4.3. Software Design

The comprehensive test platform for anti-slip evaluation mainly included testing and analysis software and real-time simulation software. The testing and analysis software included a braking system communication module, a data acquisition and transmission module, a human–machine interaction module, a network communication module, and a data storage module. Real-time simulation software mainly included a vehicle longitudinal dynamics model that could reflect the motion state of the vehicle, and a wheel–rail adhesion model that reflected the wheel–rail contact characteristics.
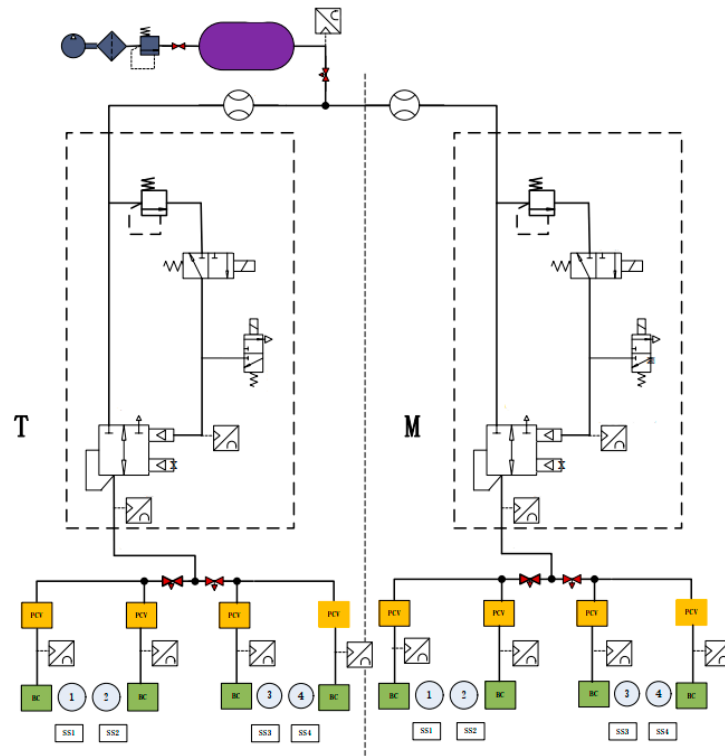
Figure 5. Design of 1M1T air braking system.

During the braking process, without paying attention to the vertical and horizontal comfort indexes of the carriage and temporarily disregarding the curve passing conditions, the performance indexes of the train braking conditions are mainly related to the longitudinal freedom of the vehicle. Therefore, the vehicle dynamics model was simplified and established, only considering its longitudinal freedom [11]. The following is a description of the dynamic equations for each submodule established based on reference [11].

(1) Wheelset

Under the rotating state of the wheelset, the main forces on the wheelset are the friction force of the brake shoe and the adhesion of the track to a single wheel. In the translational state, the force acting on the wheelset is the primary suspension force and the track adhesion force. Equations (18) and (19) respectively represent the dynamic equations for the two states.

$$I_w \cdot \ddot{\theta} = K \cdot \varphi_K \cdot R_w - F_{bw} \cdot R_w \tag{18}$$

$$M_w \cdot \ddot{x_w} = F_{fw} - F_{bw} \tag{19}$$

where M_w is the single wheel mass, I_w is the wheel moment of inertia, R_w is the vehicle radius, θ is the wheel angle, K is the equivalent clamping force, F_{bw} is the longitudinal force of the track on the single wheel, F_{fw} is the force of the primary suspension on the single wheel, and φ_K is the friction coefficient of the brake shoe.

(2) Frame

The longitudinal degrees of freedom of the frame are mainly affected by the primary and secondary suspension forces. The number of primary suspension forces is four, and the number of secondary suspension forces is two. The dynamic equation is Equation (20).

$$M_f \cdot \ddot{x}_f = 4 * F_{wf} + 2 * F_{cf} \tag{20}$$

where M_f is the mass of the frame, x_f is the longitudinal displacement of the frame, F_{wf} is the force exerted by a single primary suspension on the frame, and F_{cf} is the force exerted by a single secondary suspension on the frame.

(3) Vehicle body

The longitudinal degree of freedom of the vehicle body is mainly affected by the secondary suspension force and the coupler force. The number of secondary suspension forces is 4, and the dynamic equation is Equation (21).

$$M_c \cdot \ddot{x}_c = 4 * F_{fc} + F_{coupler1} - F_{coupler2} - F_{resistance} \tag{21}$$

where M_c is the mass of the vehicle body, x_c is the longitudinal displacement of the vehicle body, $F_{coupler1}$, $F_{coupler2}$ are the coupler forces at both ends, and $F_{resistance}$ is the basic resistance.

(4) Primary suspension force, secondary suspension force, coupler force

In the modeling of this system, the primary and secondary suspension forces, as well as the coupler forces, were simplified as spring damping mechanical models. The dynamic formulas are shown in Equations (22)–(24).

$$F_{fw} = K_{1x} \cdot \left(x_f - x_w \right) + C_{1x} \cdot \left(\dot{x}_f - \dot{x}_w \right) \tag{22}$$

$$F_{cf} = K_{2x} \cdot \left(x_c - x_f \right) + C_{2x} \cdot \left(\dot{x}_c - \dot{x}_f \right) \tag{23}$$

$$F_{coupler} = K_c \cdot \left(x_{c1} - x_{c2} \right) + C_c \cdot \left(\dot{x}_{c1} - \dot{x}_{c2} \right) \tag{24}$$

where K_{1x} is the longitudinal positioning stiffness between single wheel and frame, C_{1x} is the longitudinal damping between single wheel and frame, K_{2x} is the longitudinal positioning stiffness between single wheel and frame, C_{2x} is the longitudinal damping between single wheel and frame, K_c is the longitudinal positioning stiffness between vehicles, and C_c is the longitudinal damping between vehicles.

In the semi-physical simulation of anti-slip control, the accuracy of establishing the wheel–rail adhesion model is crucial for the construction of the test platform. This article selects the adhesion calculation model proposed by Olrich Polach [12] as the simulation model. This model can reflect the relationship between adhesion coefficient and axle load, vehicle speed, and slip rate, and is suitable for the calculation of adhesion coefficient under unstable conditions in the slipping area, i.e., slipping conditions. Both efficiency and accuracy are guaranteed, and the calculation method is shown in Equation (25) below.

$$\mu = \frac{2f_0 \left[(1 - A)e^{-Bw} + A \right]}{\pi} \left[\frac{\frac{2X\pi a^2 b}{3Q\mu}s}{1 + \left(\frac{2X\pi a^2 b}{3Q\mu}s \right)} + arctan \left(\frac{2X\pi a^2 b}{3Q\mu}s \right) \right] \tag{25}$$

In the formula above, μ is the adhesion coefficient; f_0 is the maximum friction coefficient of the wheel rail; Q is the axle load; A, B are the friction coefficient adjustment parameters, and the values of A and B can be determined from Table 9; w is the relative sliding speed; a is the length of the longitudinal half axis in the elliptical contact area between the wheel and rail; b is the length of the transverse half axis in the elliptical contact area between the wheel and rail; X is the wheel rail contact shear stiffness; s is the slip rate.

Table 9. Parameter values of adhesion model under different working conditions.

Model Parameter	Dry Rail	Wet Rail	0.08 Maximum Adhesion	0.07 Maximum Adhesion	0.06 Maximum Adhesion	0.05 Maximum Adhesion
A	0.30	0.20	0.20	0.20	0.20	0.20
B	0.60	0.60	0.10	0.10	0.10	0.10

4.4. Verification of Comprehensive Test Platform for Anti-Slip System

According to the performance requirements of EN 15595 [1] for anti-slip simulation devices, it is necessary to adjust the parameters of the vehicle and wheel–rail model, reproduce the actual vehicle slipping test conditions on the platform, and compare the actual vehicle test data to verify the accuracy and effectiveness of the platform test in simulating the actual train slipping conditions.

The dry rail test simulated the high adhesion conditions of the wheel–rail when the vehicle does not slip during normal braking. The actual speed, deceleration, braking distance, etc., obtained from the platform simulation test were compared and verified with the data obtained from the actual vehicle test or theoretical data obtained from the design parameters of the anti-slip controller. The test requirement was to simulate the braking distance under different initial speeds, and the error between the theoretical braking distance calculated based on the target deceleration plus 0.5 s of idle time was not to exceed 5%. The test results are shown in Table 10. The test results show that the error between the simulated braking distance and the theoretical braking distance under all conditions was less than 5%, and the performance met the requirements.

Table 10. Parameter values of adhesion model under different working conditions.

Brake Level	Initial Braking Speed (km/h)	Simulated Braking Distance (m)	Theoretical Braking Distance (m)	Error (%)
Maximum service braking	100	550.51	542.463	1.48
	200	2612.66	2603.54	0.35
	300	7072.84	7139.20	0.93
Fast braking	100	314.33	301.52	4.25
	200	1403.87	1367.57	2.65
	300	4015.98	3951.21	1.64
Emergency braking	100	412.66	399.70	3.24
	200	1619.55	1582.68	2.33
	300	4078.72	4015.48	1.58

The selected conditions for the actual vehicle test data were as follows. The initial speed of T vehicle collecting data was 150 km/h, and the initial speed of M vehicle collecting data was 117 km/h. The braking level was fast braking, with low adhesion conditions created by spraying antifreeze on the rail. By selecting appropriate vehicle parameters and virtual rail model parameters, the actual vehicle anti-slip test process was reproduced on the anti-slip test platform, and the simulation results were compared and verified with the actual vehicle test results according to the above three requirements. Due to the inconsistency in the collection time points of the actual vehicle test data for T and M vehicles, the simulation values of T and M vehicles were compared and verified with the actual vehicle test values.

According to the requirements of the relevant chapters in the EN 15595 on the performance verification of anti-slip simulation devices, the comparison of actual vehicle test data should be conducted under wet rail conditions. The comparison items include braking distance, speed curve, and slip rate distribution. The calculation method is detailed in the EN 15595. The test results are shown in Table 11. The test results showed that the error between the simulated braking distance and the theoretical braking distance under all conditions was less than 5%, and the performance met the requirements.

Table 11. Error statistics and mean calculation of test and simulation values.

Axle Numbers	0–5%	5–10%	10–20%	20–30%	30–40%	>50%
Error of axle 1 of T vehicle (%)	11.352	16.903	6.40172	52.4905	17.2723	0
Error of axle 2 of T vehicle (%)	6.2676	16.412	13.3894	6.47509	40.1843	0
Error of axle 3 of T vehicle (%)	2.2960	16.935	29.7074	4.08244	5.69206	0
Error of axle 4 of T vehicle (%)	36.530	14.532	20.5303	11.8072	12.8465	0
Error of axle 1 of M vehicle (%)	16.503	12.386	18.6542	19.2538	30.2981	0
Error of axle 2 of M vehicle (%)	0.4914	14.663	5.82357	26.0386	26.9687	0
Error of axle 3 of M vehicle (%)	14.316	25.224	20.6282	9.84491	9.08482	0
Error of axle 4 of M vehicle (%)	3.8996	6.3442	18.4675	23.4830	7.86394	0
Average (%)	11.457	15.425	16.7003	19.1844	18.7763	0

5. Experimental Verification of Comprehensive Evaluation Method of Train Anti-Slip System Performance

In the semi-physical simulation platform test method, the virtual rail established through numerical models can provide a standard testing environment for the anti-slip system, which not only has controllability and repeatability, but also accurately and conveniently obtains relevant physical quantities. In addition, compared to actual vehicle testing, the installation of sensors in platform testing is more convenient, providing the feasibility of measuring certain physical quantities. Therefore, the comprehensive evaluation method of train anti-slip system performance is more suitable for experimental application on a semi-physical simulation platform. Based on the evaluation method content, Table 12 summarizes the test conditions on the semi-physical simulation platform.

Table 12. Semi-physical simulation bench test conditions.

Load	Brake Level	Adhesion Conditions
AW3 / AW0	Emergency braking	Dry rail 0.08 maximum adhesion coefficient 0.07 maximum adhesion coefficient 0.06 maximum adhesion coefficient 0.05 maximum adhesion coefficient
	Maximum service braking	Dry rail 0.08 maximum adhesion coefficient 0.07 maximum adhesion coefficient 0.06 maximum adhesion coefficient 0.05 maximum adhesion coefficient

Calculation Results of Evaluation Indexes for Anti-Slip System

The comprehensive evaluation method of train anti-slip system performance should be able to reflect the performance of the same anti-slip system under multiple slipping conditions, and also have the ability to compare different anti-slip systems horizontally (the differences in anti-slip systems are mainly reflected in anti-slip control strategies or air brake system parameters and components). Therefore, on the semi-physical simulation platform, based on the same air braking system, the anti-slip control strategies under the following two different speed difference criteria were tested, as shown in Table 13. The table shows the speed difference between the vehicle speed and axle speed represents the axle deceleration, and points A, B, and C represent the control points in the anti-slip control strategy that control the slipping of the wheelset [13]. Each control point corresponds to a detection criterion and action status. For example, under AW3 working condition, the train load is 57,780 kg, AW0 is 49,580 kg, and the initial braking speed is 200 km/h.

Table 13. Different anti-slip control strategies.

Test Object	A-Point Criterion	B-Point Criterion	C-Point Criterion
Anti-slip control strategy 1	$\Delta v > 6 \, \mathrm{km/h} \& \beta < -3 \, \mathrm{km/h/s}$	$\beta > 0 \, \mathrm{km/h/s}$	$\Delta v < 4 \, \mathrm{km/h}$
Anti-slip control strategy 2	$\Delta v > 3 \, \mathrm{km/h} \& \beta < -3 \, \mathrm{km/h/s}$	$\beta > 0 \, \mathrm{km/h/s}$	$\Delta v < 4 \, \mathrm{km/h}$

We calculated the various parameters required for evaluating the performance of the anti-slip system, and some of the calculation results are shown in Figure 6. Selecting the calculation results of adhesion coefficient utilization, air consumption increase ratio, wheelset slipping energy, and average anti-slip valve action frequency under AW0 and maximum service braking conditions, it can be seen from Figure 6a that the adhesion coefficient utilization of anti-slip control strategy 1 was higher than that of anti-slip control strategy 2. Under this index, anti-slip control strategy 1 was better, while Figure 6c shows that the wheelset slipping energy of anti-slip control strategy 1 was higher than that of anti-slip control strategy 2. This also led to the poor performance of anti-slip control strategy 1 compared to anti-slip control strategy 2 in terms of the wheelset slipping energy index. Therefore, it can be found that a single evaluation index has difficulty in reflecting the performance of anti-slip system. Therefore, the establishment of a comprehensive evaluation method for anti-slip control is necessary.

(**a**) Adhesion coefficient utilization

(**b**) Air consumption increase ratio

(**c**) Wheelset slipping energy

(**d**) Average anti-slip valve action frequency
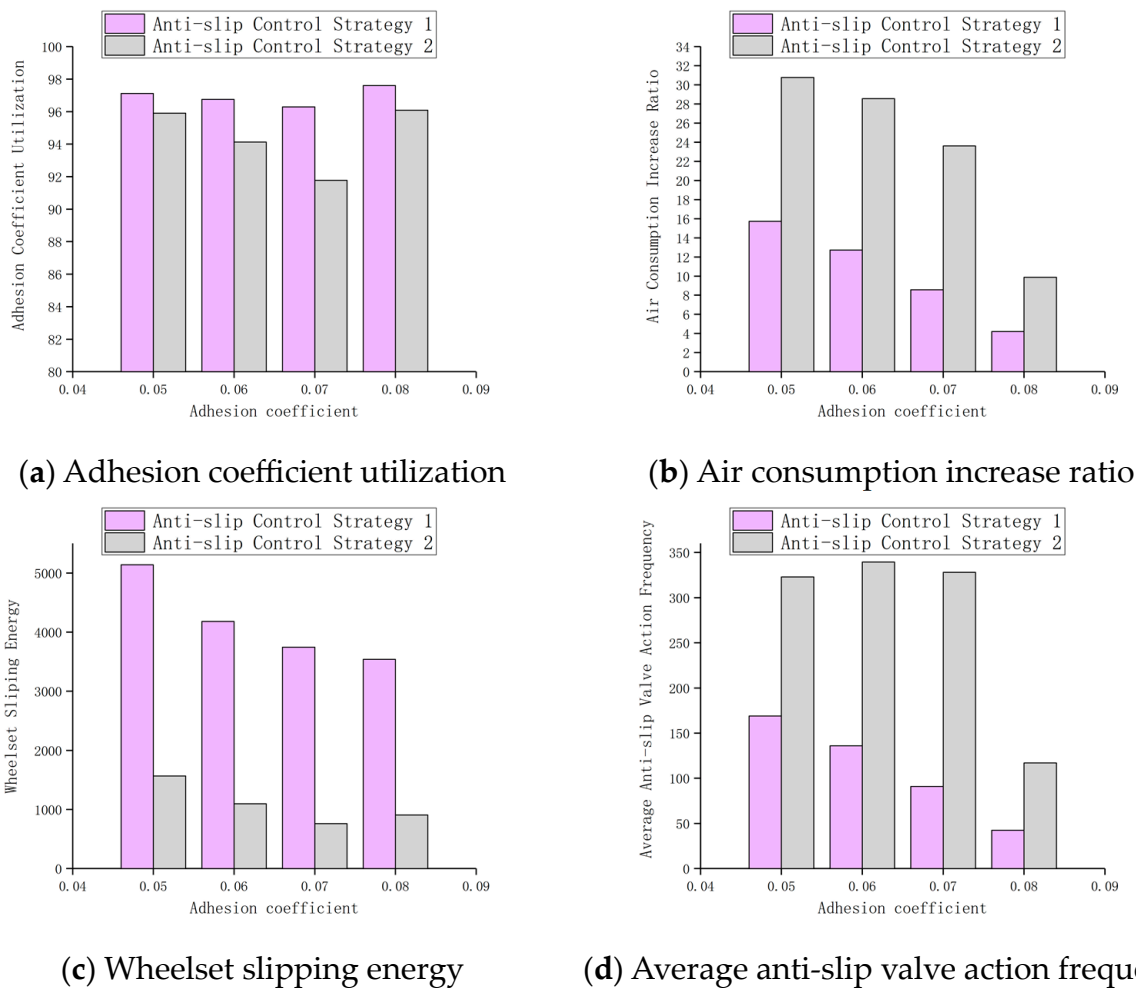
Figure 6. Comparison of partial calculation results (AW0 and maximum service brake) for different anti-slip control strategies.

Load and braking level are important factors that affect train anti-slip control. In the anti-slip evaluation method of this article, a braking level layer and a load layer were added. From the calculation results shown in Figure 7a, it can be seen that there was a significant difference in wheelset slipping energy between AW3 and AW0 under emergency braking, and from the calculation results shown in Figure 7b, there was also a significant difference in wheelset slipping energy between emergency braking and maximum service braking under AW3 conditions. Therefore, it was necessary to add a load layer and a braking level layer to the comprehensive evaluation method of train anti-slip system performance.
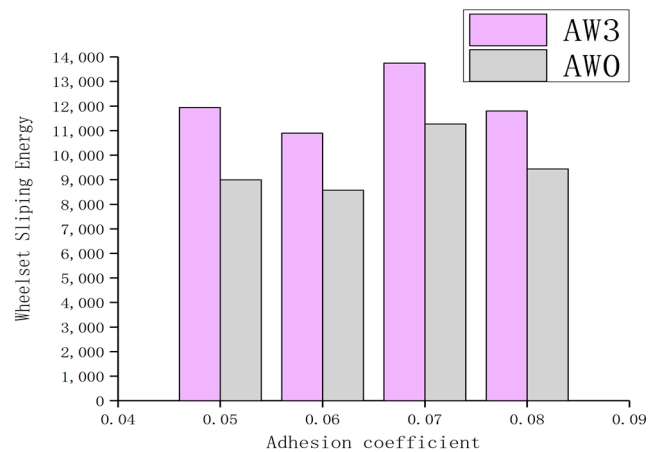
(**a**) AW3 and AW0 under emergency braking
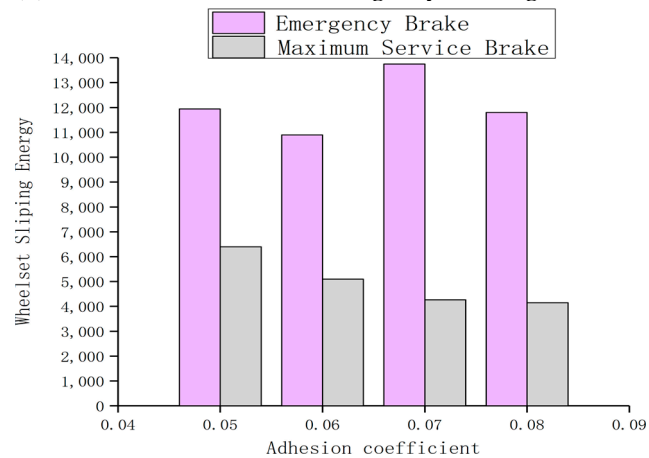
(**b**) Emergency brake and maximum service braking under AW3

Figure 7. Comparison of wheelset slipping energy under different loads and braking levels.

6. Discussion

Taking the test results of anti-slip control strategy 1 as an example, radar charts of the anti-slip performance indexes of AW3 and AW0 trains under different braking levels and adhesion conditions were plotted, as shown in Figures 8 and 9.

For the adhesion coefficient utilization index, this anti-slip strategy performed well in all working conditions, fully utilizing adhesion and shortening the braking distance under slipping conditions.

The air consumption increase ratio index value was greatly influenced by the adhesion conditions. The maximum adhesion coefficient increased from 0.05 to 0.08 in sequence, and the air consumption increase ratio index gradually increased. This indicates that improving the adhesion coefficient can reduce the degree of compressed air consumption in the anti-slip control process. Under the same load and adhesion coefficient conditions, the air

consumption increase for maximum service braking was better than the performance index for emergency braking, while changing the load had little impact on the air consumption increase of this anti-slip system. Overall, this anti-slip control strategy had the worst performance in terms of air consumption increase ratio under AW0, emergency braking, and 0.05 maximum adhesion coefficient conditions, with a value of 0.4784. The optimal air consumption increase ratio was 0.9057 under AW0, maximum service braking, and 0.08 maximum adhesion coefficient conditions.
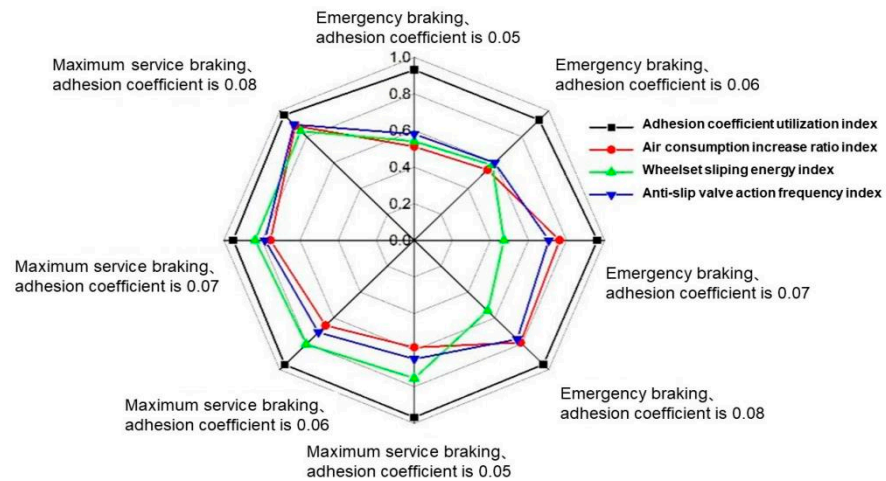
Figure 8. Index results under various working conditions under AW3.
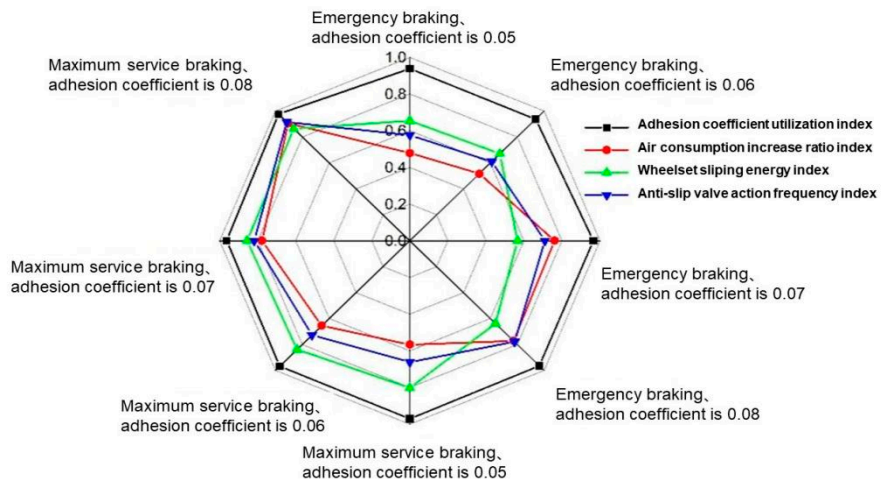
Figure 9. Index results under various working conditions under AW0.

The wheelset slipping energy index was mainly influenced by the braking level and load, especially the braking level. When the braking level was the maximum service braking, the wheelset slipped less, and the wheelset slipping energy index was significantly higher than the calculated value under the emergency braking level. This index was the worst under AW3, emergency braking, and 0.07 maximum adhesion coefficient conditions, with a value of 0.4712. The optimal condition was 0.8638 under AW0, maximum service braking, and 0.08 maximum adhesion coefficient.

With the anti-slip valve action frequency index, as the parameters of the air braking system did not change, the results of this index were similar to the air consumption increase ratio index under different working conditions. The performance of the anti-slip valve action frequency was the worst under AW0, emergency braking, and 0.05 maximum adhesion coefficient working conditions, with a value of 0.576. The optimal performance of the anti-slip valve action frequency was 0.915 under AW0, maximum service braking, and 0.08 maximum adhesion coefficient working conditions.

Based on the index results under all working conditions, combined with the hierarchical system of anti-slip system performance evaluation and the weight coefficients of each layer element established in the previous text, the comprehensive evaluation results of the anti-slip system performance under two control strategies were calculated, and finally the comprehensive evaluation index calculation results of the two anti-slip control strategies were obtained. The anti-slip performance evaluation result R1 of anti-slip control strategy 1 was 0.8389, while the anti-slip performance evaluation result R2 of anti-slip control strategy 2 was 0.7912. Therefore, overall, the former had better anti-slip performance than the latter.

7. Conclusions

This article addresses the problem of single and simplistic evaluation indexes for train anti-slip control, and proposes a comprehensive evaluation method based on the analytic hierarchy process by adding a load layer and a braking level layer. This evaluation method for train anti-slip systems uses an adhesion coefficient utilization index, an air consumption increase ratio index, a wheelset slipping energy index, and an anti-slip valve action frequency index, which enhances the comprehensiveness and scientific basis of evaluation.

To accurately simulate the operating environment of trains, this article establishes a semi-physical simulation platform for anti-slip control by developing vehicle models, adhesion models, and physical design of braking air circuits. The platform was validated, providing a simulation platform for implementing anti-slip strategies.

Based on the constructed semi-physical simulation platform for anti-slip control, this article conducted a series of performance tests on anti-slip control strategies. A multi-dimensional comprehensive evaluation was conducted on the anti-slip control performance of two anti-slip strategies under different loads, brake levels, and adhesion coefficient levels. The results showed that the R1 and R2 values of the two anti-slip control strategies under complex working conditions were 0.8389 and 0.7912, respectively. Therefore, it can be clearly shown that the control effect of anti-slip control strategy 1 was better than that of anti-slip control strategy 2.

The model used in the semi-physical simulation platform established in this article is based on the POLACH theory [12]. In subsequent research, it was found that the theory ignored the adhesive improvement effect. Therefore, in further research, more accurate adhesive models can be used to update the semi-physical simulation platform and comprehensive evaluation methods established in this article, which is an important research direction in the future.

References

1. *BS EN 15595*; Railway Applications Braking Wheel Slide Protection. European Committee for Standardization: Brussels, Belgium; CEN Management Centre: London, UK, 2009.
2. *UIC CODE 541-05*; 2nd ed. Brake—Specifications for the Construction of Various Brake arts—Wheel Slide Protection Device (WSP). International Union of Railways: Paris, France, 2005.
3. *TB/T 3009-2011*; Anti-Skid Device for Railway Passenger Car and Powered Car Train-Set. China Academy of Railway Sciences, Institute of Rolling Stock: Beijing, China, 2012.
4. Wu, Z.; Hu, Y.; Shen, G.; Zhu, X. Practical Study on the Efficiency of Anti-Slip & Slide System for Metro Vehicle. *Urban Mass Transit* **1998**, *2*, 32–34.
5. Chen, W.; Zhou, J.; Wang, X.; Cao, H.; Han, X. Theory and Test of Wheel–slide–protection System in Brake Control of China EMU. *Railw. Locomot. Car* **2011**, *31*, 32–37.
6. Li, Y. The Antiskid Control Method for Air Braking on Urban Rail Vehicles. *Roll. Stock.* **2011**, *49*, 38–40+6.
7. Hijikata, D.; Peng, H. WSP performance evaluation using stopping distance distribution by simulation. *Foreign Railw. Locomot. Mot. Car* **2020**, *6*, 9–14.
8. Diao, F.; Zhu, W.; Qin, L.; Wu, M. Evaluation Method of Anti-Sliding Control Based on Analytic Hierarchy Process. *Open J. Transp. Technol.* **2018**, *7*, 371–380.
9. Ge, P.; Boiteux, M. The effect of sliding energy on brake adhesion. *Foreign Roll. Stock.* **1991**, *5*, 47–53+9.
10. Guo, J.; Zhang, Z.; Sun, Q. Study and Applications of Analytic Hierarchy Process. *China Saf. Sci. J.* **2008**, *5*, 148–153.
11. Hu, Y. *Dynamics of Modern Rail Vehicles*; China Railway Publishing House: Beijing, China, 2009; pp. 61–91.
12. Polach, O. Creep force in simulations of traction vehicles running on adhesion limit. *Wear* **2005**, *258*, 992–1000. [CrossRef]
13. Li, W. Simulation on Anti-Sliding Control of Emu Braking System. Master's Thesis, Southwest Jiaotong University, Chengdu, China, 2012.